

**Phase stability, porosity distribution and microstructural evolution of amorphous Al<sub>50</sub>Ti<sub>50</sub> powders consolidated by electrical resistance sintering**

P. Urban, F. G. Cuevas, J. M. Montes, and J. Cintas

Citation: [AIP Conference Proceedings](#) **1653**, 020100 (2015); doi: 10.1063/1.4914291

View online: <http://dx.doi.org/10.1063/1.4914291>

View Table of Contents: <http://scitation.aip.org/content/aip/proceeding/aipcp/1653?ver=pdfcov>

Published by the [AIP Publishing](#)

---

**Articles you may be interested in**

[Consolidation of Bi-2223 superconducting powders by spark plasma sintering](#)

J. Appl. Phys. **112**, 113906 (2012); 10.1063/1.4768257

[Microstructural evolution of triple junction and grain boundary phases of a Nd-Fe-B sintered magnet by post-sintering annealing](#)

J. Appl. Phys. **109**, 07A703 (2011); 10.1063/1.3561805

[Effect Of Milling Time On Microstructure Of Mechanically Alloyed Al-Ti Powders](#)

AIP Conf. Proc. **1202**, 117 (2010); 10.1063/1.3295580

[Structural evolution of mechanical alloyed Fe-Al powders after consolidation and thermal ageing](#)

J. Appl. Phys. **74**, 2053 (1993); 10.1063/1.354769

[Mechanical properties and microstructure of sintered PVC powder. I. Elastic properties and porosity](#)

J. Appl. Phys. **48**, 1899 (1977); 10.1063/1.323946

---

# Phase Stability, Porosity Distribution and Microstructural Evolution of Amorphous Al<sub>50</sub>Ti<sub>50</sub> Powders Consolidated by Electrical Resistance Sintering

P. Urban<sup>1, a)</sup>, F. G. Cuevas<sup>2, b)</sup>, J. M. Montes<sup>1</sup> and J. Cintas<sup>1</sup>

<sup>1</sup>University of Seville, Department of Mechanical and Materials Engineering, ETSI, Camino de los Descubrimientos s/n, Seville, 41092, Spain,

<sup>2</sup>University of Huelva, Department of Chemistry and Materials Science, ETSI, Campus La Rábida, Carretera Palos s/n, Palos de la Frontera, Huelva, 21819, Spain,

<sup>a)</sup> purban@us.es

<sup>b)</sup> fgcuevas@dqcm.uhu.es

**Abstract.** The effect of intensity and duration of the electrical resistance sintering process on the phase stability, porosity distribution and microstructural evolution of Al<sub>50</sub>Ti<sub>50</sub> amorphous powders is studied. The phase transformations during the consolidation process were determined by X-ray diffraction. The porosity distribution was observed by optical and scanning electron microscopy. The amorphous phase is partially transformed to the crystalline phase during the sintering process, and formation of AlTi and AlTi<sub>3</sub> intermetallic compounds occurs for temperatures higher than 300 °C. Finally, it is observed that the compacts core have lower porosity and a higher tendency to the amorphous-crystalline phase transformation than the periphery.

**Keywords:** Amorphization, Mechanical alloying, Electrical resistance sintering, Al-Ti alloys

**PACS:** 61.43.Dq

## INTRODUCTION

The direct use of electricity as a powder sintering method has been suggested numerous times throughout the twentieth century, and still remains a topic of special interest. Among the many methods, perhaps the simplest consists in a current passing through a conductive mass of powders that is simultaneously compressed. Heat is generated by the powder itself due to the Joule effect. This technique was already described in 1933 by Taylor<sup>[1]</sup> but no systematic study was carried out until some years later by Lenel<sup>[2]</sup>, who called it “Electrical resistance sintering” (ERS). Among the advantages of the ERS method<sup>[3]</sup>, as compared with the conventional route of cold pressing and furnace sintering, we can mention: the use of relatively low pressures (about 80 MPa) to achieve very high densification, the use of extremely short processing times (about one second), and the possibility of sintering without protective atmospheres. The most important drawbacks are operating problems and an inhomogeneous temperature distribution in the powder mass.

## MATERIALS AND EXPERIMENTAL PROCEDURE

Pure elemental powders of Ti Se-Jong 4 (purity > 99.4 %) and Al AS61 (purity > 99.7 %) were mixed to give the atomic compositions of  $Ti_{50}Al_{50}$ . The mix was poured and sealed in a cylindrical 304 stainless steel vial, with 304 stainless steel balls and 1.5 wt. % of wax. The wax acts as the process control agent to balance the welding and fracture processes. The mix was then dry-milled at 25 °C for 75 hours in a high energy attritor ball mill (the ball-to-powder weight ratio was 50:1, the rotor speed was 500 rpm and the protective atmosphere was purified argon) to obtain an amorphous structure<sup>[3]</sup>. The electrical requirements of the process (high intensity and low voltage) are fulfilled by an appropriate resistance welding machine, which also can provide the necessary compressive mechanical stress.. The machine consists of a single phase transformer of 100 kVA, a pneumatic cylinder capable of providing a force of 1.400 kgf and an electronic controller that governs the process sequences and regulates the current intensity. The powder container die was made with an alumina pipe enclosed by a metallic hoop. The die had an orifice of 12 mm in diameter to host the powder. The die is closed on the top and bottom orifices with punches of temperature resistance cooper. The powder mass to be sintered is located between those punches. Two wafers of an electrical erosion resistant alloy (75.3%W-24.6%Cu) are located in direct contact with the powder. They have the function, due to their small thermal conductivity, of interrupting the flow of heat generated in the powder mass towards the water cooled electrodes (Figure 1). The phase transformations and microstructural evolution during the consolidation process were determined by X-ray diffraction (XRD, Siemens D500). The porosity distribution was observed by optical microscopy (Nikon Epiphot 200) and scanning electron microscopy (SEM, Philips XL 30).

## RESULTS AND DISCUSSION

### Final Porosity

In general, powders sintered with low intensity have high porosity (Figure 2) and low density. By increasing the intensity, the material increases its compacting capacity by reducing the number of pores between particles. Increasing processing time (in cycles in Figure 2) has similar consequences, although for the studied values the influence of intensity is more remarkable.

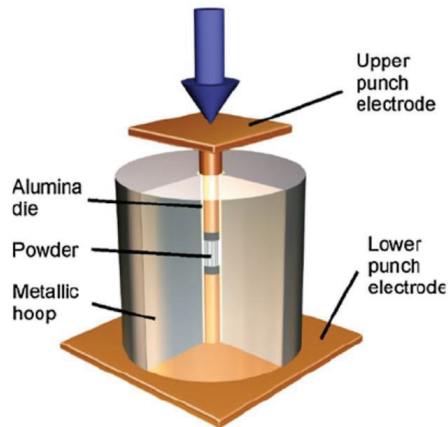


**Figure 1.** Sketch of punches and die used in electrical resistance sintering.

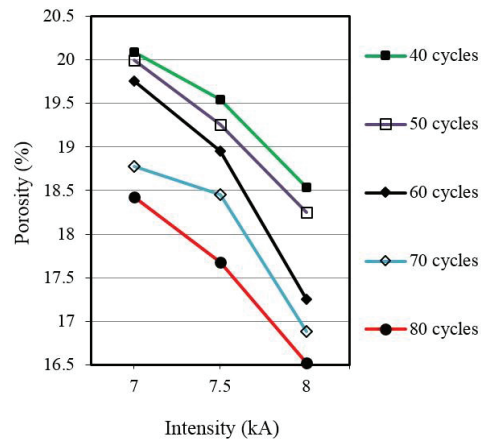


**Figure 2.** Final porosity vs. intensity of the specimens after the ERS for different processing times.

As expected, the achievement of an amorphous structure (hardened particles by mechanical alloying), makes more difficult to eliminate the porosity than in the case of ductile, crystalline and non-mechanical alloyed powders. In the first stage of the ERS process (pressing stage at 80 MPa), the porosity of the amorphous powders decreases less compared to the second stage of the ERS process (action of the electric current). No satisfactory experiments have been carried out with lower and higher intensities. For lower intensities, the powder, having a high electrical resistivity, do not sinter. For higher intensities, mechanically alloyed powders adhere to wafers, resulting impossible to separate the compact from the wafers.

### Optical And Scanning Electron Microscopy

ERS compact with 7 kA and 40 cycles (ERS 7/40) have been chosen to perform a metallographic analysis regarding the influence of sintering on the microstructure. The uniform porosity distribution of conventionally processed compacts is clearly different from the non-uniform distribution of the electrical processed ones. Electrically sintered compacts have a densified core (Figure 3.a) and a more porous periphery (Figure 3.b), as can be seen by optical microscopy in metallographically prepared and non-etched compacts. Very irregular distribution for the core (Figure 4.a) and the periphery (Figure 4.b) of the compact can also be observed by SEM. The different porosity is due to an uneven temperature distribution inside each compact, due both to the behaviour of the electric current inside the material, and the cooling effect of the die walls. The temperature rise is smaller, and cooling is faster, nearer the die wall. The different temperature distribution in the compact could also affect the proportion of amorphous phase. The areas near the axis of the cylindrical compact could transform to a crystalline phase whereas the zones closer to the die wall could remain as an amorphous phase.

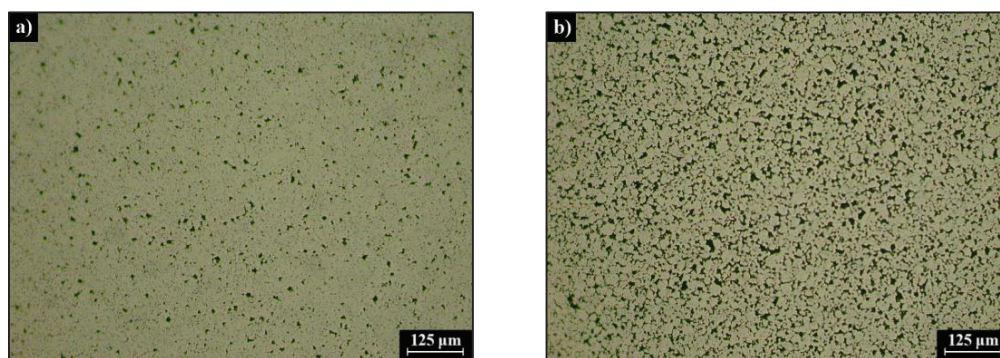


**Figure 3.** Porosity (optical microscopy) in  $\text{Al}_{50}\text{Ti}_{50}$  compact ERS 7/40. (a) Core and (b) periphery of the compact.

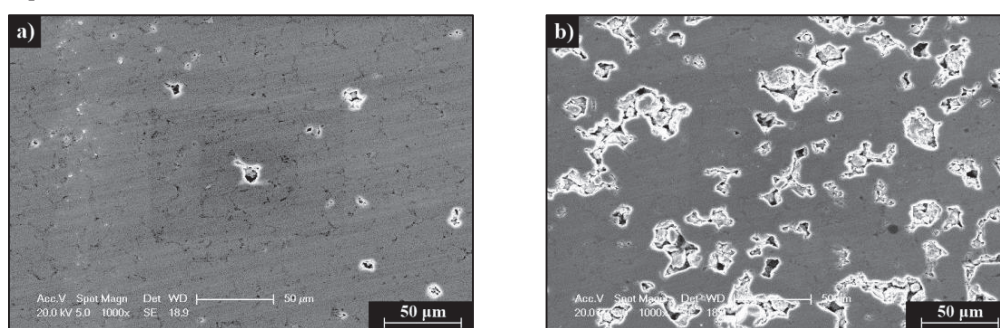


**Figure 4.** Distribution of porosity (SEM) in  $\text{Al}_{50}\text{Ti}_{50}$  compact ERS7/40. (a) Core and (b) periphery of the compact.

## X-Ray Diffraction

The evolution of the amorphous-crystalline transformation with the temperature rise in the ERS compacts can be evaluated by X-ray diffraction (Figure 5). At room temperature, after the electrical sintering of the amorphous powders, a small peak, belonging to a small amount of the  $\text{AlTi}$  and/or  $\text{AlTi}_3$  intermetallic compounds, appears. If the compact is heated, the peak begins to grow, which implies an increase of the crystalline phase and decrease of the amorphous phase. At 300 °C, the main peak (39°) shows the almost complete crystallization, because at higher temperatures (500 and 600 °C) there is no big difference between the main peaks. Besides, above 300 °C, other secondary peaks (45, 66, 78 and 79°) appear for the same compounds. For all XRD patterns, it should be considered that there is more crystalline phase in the core of the compact and more amorphous phase in the periphery. The pattern register the sum of the amorphous and the crystalline phase along the entire section of the compact. Finally, it may be mentioned that sintered compacts are thermally unstable to relatively low temperatures, because heating at 300 °C promotes almost the completely crystalline of the amorphous phase. Itsukaichi et al.<sup>[4]</sup> showed that an  $\text{Al}_{50}\text{Ti}_{50}$  amorphous alloy can be consolidated by hot pressing with temperature of 800 °C and pressure of 100 MPa for 600 s and this amorphous phase crystallize to an  $\text{AlTi}$  intermetallic compound. Calderon et al.<sup>[5]</sup> consolidated  $\text{Al}_{50}\text{Ti}_{50}$  amorphous alloy by spark plasma sintering to form two intermetallic compounds,  $\text{AlTi}$  and  $\text{AlTi}_3$ .

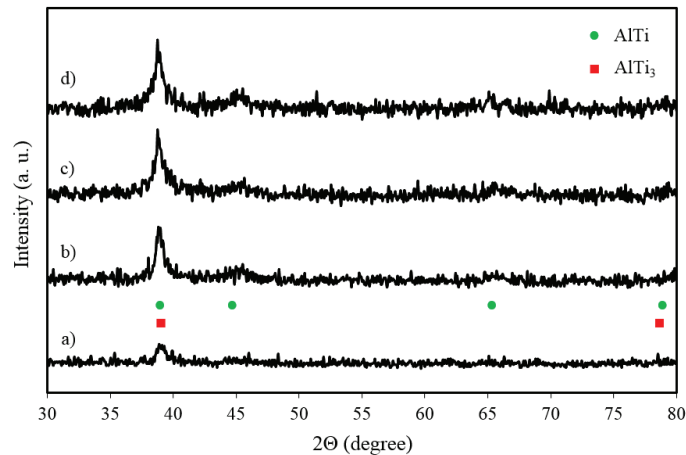


**Figure 5.** XRD patterns of ERS (7/40)  $\text{Al}_{50}\text{Ti}_{50}$  compact heated up to (a) 25, (b) 300, (c) 500 and (d) 650 °C.

## CONCLUSIONS

Al and Ti particles, milled for 75 hours, have high hardness and oxidize very easily forming a layer of oxides with very high electrical resistivity. Because of the high hardness and small plastic deformation ability, it results very difficult to conventionally press and sinter the powders. Furthermore, because of the oxide layers, it is very difficult to sinter powders electrically, and the current is capable to overpass only a small amount of powder in the matrix. Sintered compacts with different intensities and times of processing exhibit a porosity between 16.5 and 20%. The amorphous structure of the powders milled for 75 hours is partially lost after ERS, and a complete amorphous-crystalline transformation occurs around 300 °C.

## ACKNOWLEDGMENTS

Financial support of the “Ministerio de Economía y Competitividad” (Spain) through the research project DPI2012-37948-C02-01 is gratefully acknowledged.

## REFERENCES

1. G. F. Taylor, U.S. Patent No. 1,896,854 (7 February 1933).
2. F. V. Lenel, *J. Met.* 7, 158-167 (1955).
3. J. M. Montes, J. A. Rodríguez and E. J. Herrera, *Rev. Metal. Madrid* 39, 99-106 (2003).
4. T. Itsukaichi, K. Masuyama, M. Umemoto and I. Okane. *J. Mater. Res.* 8, 1817-1828 (1993).
5. H.A. Calderón, V. Garibay-Feblés and M. Yamaguchi. *Mater. Sci. Eng. A* 329-331 196-205 (200)